JACS
JOURNAL OF THE AMERICAN CHEMICAL SOCIETY

Communication

pubs.acs.org/JACS

Role of Coherent Low-Frequency Motion in Excited-State Proton Transfer of Green Fluorescent Protein Studied by Time-Resolved Impulsive Stimulated Raman Spectroscopy

Tomotsumi Fujisawa,[†,∥,⊥] Hikaru Kuramochi,[†,⊥] Haruko Hosoi,[‡] Satoshi Takeuchi,[†,§] and Tahei Tahara*[,†,§]

[†]Molecular Spectroscopy Laboratory, RIKEN, and [§]Ultrafast Spectroscopy Research Team, RIKEN Center for Advanced Photonics (RAP), 2-1 Hirosawa, Wako 351-0198, Japan

[‡]Department of Biomolecular Science, Faculty of Sciences, Toho University, 2-2-1 Miyama, Funabashi 274-8510, Japan

Supporting Information

ABSTRACT: Green fluorescent protein (GFP) from jellyfish *Aequorea victoria*, an essential bioimaging tool, luminesces via excited-state proton transfer (ESPT) in which the phenolic proton of the *p*-hydroxybenzylideneimidazolinone chromophore is transferred to Glu222 through a hydrogen-bond network. In this process, the ESPT mediated by the low-frequency motion of the chromophore has been proposed. We address this issue using femtosecond time-resolved impulsive stimulated Raman spectroscopy. After coherently exciting low-frequency modes (<300 cm^{-1}) in the excited state of GFP, we examined the excited-state structural evolution and the ESPT dynamics within the dephasing time of the low-frequency vibration. A clear anharmonic vibrational coupling is found between one high-frequency mode of the chromophore (phenolic CH bend) and a low-frequency mode at ∼104 cm^{-1}. However, the data show that this low-frequency motion does not substantially affect the ESPT dynamics.

Due to the genetically encodable property, fluorescent proteins are now indispensable bioimaging tools for visualizing gene expression and protein function in living cells.[1−4] Green fluorescent protein (GFP) from the jellyfish *Aequorea victoria* is the origin of the fluorescent protein family, and its properties have been intensively studied so far.[1−7] In its *β*-barrel motif, GFP encloses the intrinsic chromophore, *p*-hydroxybenzylideneimidazolinone, which is formed autocatalytically from the Ser65-Tyr66-Gly67. The chromophore is nonfluorescent when isolated, but it fluoresces brightly in the protein pocket of GFP which suppresses the nonradiative deactivation process.[5]

The photophysics of GFP has been studied for two decades from dynamical and structural aspects.[1,6−16] Inside GFP, the chromophore is found in the cis isomer which is either protonated or deprotonated.[1] The major population in the physiological condition is in the protonated state (A form) that exhibits a main absorption band at ∼398 nm, and excitation of the A form yields green fluorescence with a large Stokes shift (∼5440 cm^{-1}).[1] The time-resolved fluorescence study clarified that photoexcitation of the A form triggers excited-state proton transfer (ESPT), producing the green-fluorescent deprotonated chromophore (I form) in the excited state (Figure 1A) on the picosecond time scale.[8] X-ray crystallography revealed that the hydrogen-bond chain for the proton transfer links the phenolic hydroxyl group of the chromophore, water, Ser205, and Glu222.[9−11] Consistently, ultrafast IR studies proved the concurrent protonation of the terminal proton acceptor Glu222 as the ESPT proceeds.[14−16] After emission of the green fluorescence, most of the I-form molecules are reprotonated and relax back to the original A form.[8,13]

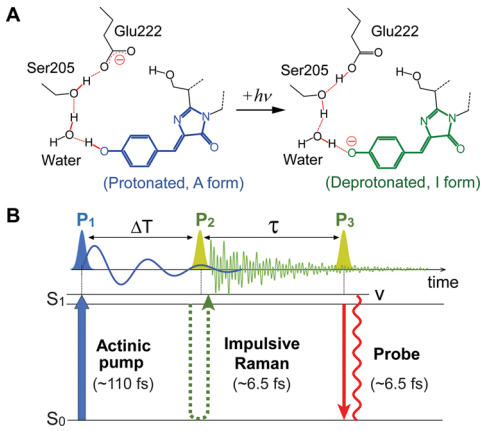

Figure 1. (A) Excited-state proton transfer in GFP.[11] (B) Experimental scheme of TR-ISRS.

Recently, the importance of a low-frequency motion in the ESPT was proposed on the basis of ultrafast Raman measurements.[17] In the study, Fang et al. used femtosecond stimulated Raman spectroscopy (FSRS) and measured time-resolved Raman spectra of the A* form (* denotes the excited state). They found the oscillatory modulation (period: ∼ 0.28 ps) in both frequencies and intensities of multiple high-frequency bands of the A* form and attributed it to the anharmonic vibrational coupling with a coherently excited low-frequency vibration of the chromophore. Furthermore, they proposed that this low-frequency mode is the phenolic wag motion that

Received: October 21, 2015
Published: March 4, 2016

DOI: 10.1021/jacs.5b11038
J. Am. Chem. Soc. 2016, 138, 3942−3945

modulates the hydrogen-bond interactions for the ESPT, facilitating the ESPT reaction. This interpretation is very stimulating, but the low-frequency mode that modulates high-frequency vibrations was not observed with sufficient clarity, and more importantly, the product formation was not monitored. Therefore, the importance of the coherent low-frequency motion in the ESPT is still an open question.

Here, we use time-resolved impulsive stimulated Raman spectroscopy (TR-ISRS) to examine the role of low-frequency modes in the ESPT of wild-type GFP, by directly monitoring the excited-state structural dynamics of the A* and I* forms. In TR-ISRS, photoreaction is started by a femtosecond pump, and the Raman-active vibrations of transients are measured as the time-domain impulsive Raman signal. This ultrafast time-domain coherent Raman technique has been successfully utilized for studying the ultrafast structural dynamics occurring on the femtosecond time scale.[18−22] In particular, use of sub-7 fs pulses enables us to observe molecular vibrations up to ∼3000 cm^{-1} directly in the time domain.

The experimental scheme is illustrated in Figure 1B. First, GFP is photoexcited by the actinic pump (P_1, 110 fs, 390 nm) to prepare the population of the A* form. Then, after a variable delay time of ΔT, the impulsive Raman excitation is carried out using a pulse (P_2, sub-7 fs, 520−700 nm) that is in resonance with stimulated emission and $S_n \leftarrow S_1$ absorption of the A* form as well as the stimulated emission of the I* form. Then, the probe pulse (P_3, sub-7 fs, 520−700 nm) monitors the coherent nuclear motion of the excited states through the intensity modulation of the transient signal by changing the P_2−P_3 time interval, τ. By avoiding spectral overlap between the P_3 pulse and the ground-state absorption (Figure S1), the signal from the excited state is selectively probed. We note that the pulse duration of the actinic pump (∼110 fs) is set short enough to coherently excite low-frequency vibrational modes (<∼300 cm^{-1}) in the A* form. Therefore, in this experiment, the excited-state structural evolution as well as the ESPT dynamics can be examined while the A* form coherently vibrates with low-frequency modes.

In Figure 2A, the pump−probe signal of GFP (pH 8.0, in H_2O) measured without the impulsive Raman pulse (P_2) is depicted in black. Immediately after photoexcitation, the net signal from the A* form is close to zero because the spectral range of the probe pulse covers both the stimulated emission and the $S_n \leftarrow S_1$ absorption so that they cancel each other in the pump−probe signal (Figure S1). As time proceeds, the signal exhibits the gradual growth of the stimulated emission on the picosecond time scale, reflecting the formation of the I* form with the ESPT. In the pump−probe signal, the oscillatory feature which dephases in ∼1 ps is evident, showing that low-frequency coherent nuclear motions are actually induced in the A* form by the actinic pump. Fourier transform of this oscillatory feature (inset) reveals the low-frequency vibrational spectrum of the A* form including the prominent bands at 59, 105, and 211 cm^{-1}. Irradiation with the P_2 pulse at ΔT after the actinic pump induces the coherent nuclear motion in the A* and I* forms, as well as the decrease in the excited-state populations due to the population transfer through the $S_1 \rightarrow S_0$ (and $S_1 \rightarrow S_n$) transitions. This P_2-induced absorbance change (Figure 2, yellow area) is the TR-ISRS signal. Note that, at ΔT < 1 ps, the TR-ISRS signal is obtained while the A* form coherently vibrates with low-frequency modes. The TR-ISRS data measured at selected ΔT delay times are shown in Figure 2B. The clear oscillations represent the time-domain vibrational signals from the excited states at the ΔT delay times. After subtraction of the slowly

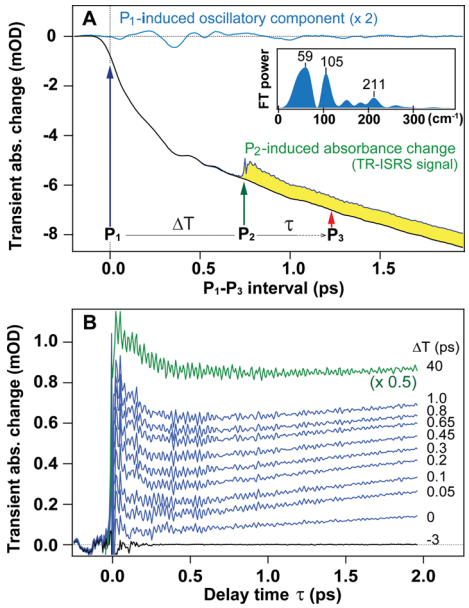

Figure 2. (A) Pump−probe (black) and TR-ISRS signals (yellow area, ΔT = 0.75 ps) of wild-type GFP (pH 8.0, in H_2O). The Fourier transform power spectrum of the oscillatory component of the pump−probe trace is shown in the inset. (B) TR-ISRS signals at selected ΔT time delays.

varying population component, the time-resolved excited-state vibrational spectra of GFP are obtained through Fourier transform analysis (Figure S2).

Figure 3 shows the time-resolved vibrational spectra of GFP (ΔT = 0−1 ps and 40 ps) obtained by TR-ISRS. Upon photoexcitation, e.g., at ΔT = 0.1 ps, the vibrational bands attributed to the A* form are clearly observed in 500−1600 cm^{-1}.[23] These bands are assignable to phenol ring deformation (1322 cm^{-1}), phenolic CO stretch (1240 cm^{-1}), phenolic CH bend (1142 cm^{-1}), exocyclic C=C−C bend (820 and 888 cm^{-1}), and imidazolinone ring deformation (601 cm^{-1}).[24,25] They exhibit different frequencies from those in the steady-state stimulated Raman spectrum of GFP (Figure S3), confirming that TR-ISRS indeed observes the vibrational modes of the excited states selectively (see details in SI).

As ΔT increases, the rise of the C=C−C bend at 820 cm^{-1} and the appearance of a new vibrational band at ∼1295 cm^{-1} are clearly observed in the time-resolved spectra. These spectral changes arise from the formation of the deprotonated I* form by the ESPT. The appearance of the vibrational mode at ∼1295 cm^{-1} was first observed in the femtosecond time-resolved IR study[14] and was later assigned to the phenolate CO stretch of the deprotonated I* form by FSRS.[17] With TR-ISRS, this band is observed with much higher S/N, which allows us to quantitatively examine its temporal behavior. The amplitude of this band grows biexponentially with the time constants of ∼2 and ∼8 ps as the ESPT proceeds (Figure S5), being consistent with previous time-resolved absorption and fluorescence studies.[8,12] Note that we do not observe any noticeable signals of the I* form at ΔT = 0 ps, negating direct generation of the I* state from the ground-state A form.[12,26] At ΔT = 40 ps when the ESPT completes, the time-resolved spectrum fully represents the I* state, showing the strong phenolate CO stretch band at ∼1300 cm^{-1}. As shown in Figure 3, the phenolate CO stretch of the I* form initially appears at 1290−1296 cm^{-1} at ΔT < 1 ps, but the frequency upshifts to 1301 cm^{-1} at ΔT = 40 ps. This frequency

DOI: 10.1021/jacs.5b11038
J. Am. Chem. Soc. 2016, 138, 3942−3945

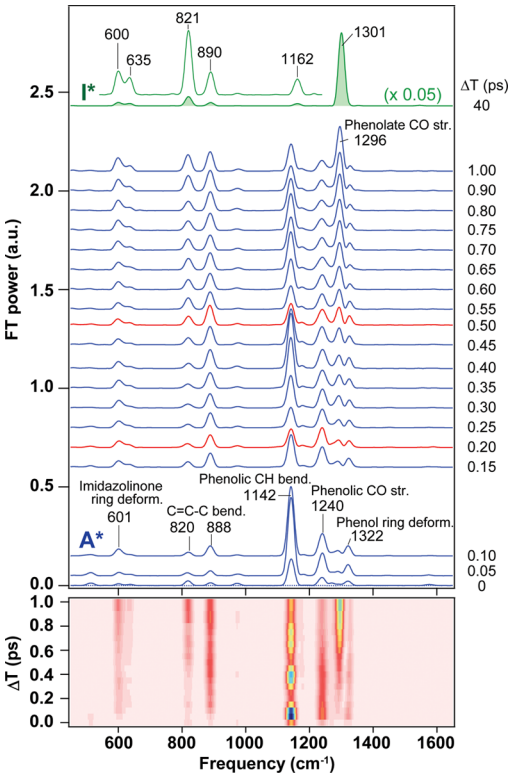

Figure 3. Time-resolved vibrational spectra of wild-type GFP (ΔT = 0–1 and 40 ps), as well as their 2D representation, obtained from Fourier transform analysis of the TR-ISRS signals. The assignments of the vibrational bands are also shown.

change with ~1 ps time constant (Figure S3) presumably reflects the vibrational cooling of the hot I* form immediately after the conversion from the A* form by the ESPT (see SI for details).[12]

In the A* and I* forms, the exocyclic C═C−C bend (~820 and ~890 cm^{-1}) and imidazolinone vibration (~600 cm^{-1}) have almost the same frequencies. On the other hand, the phenolate CH bend (1162 cm^{-1}) and the CO stretch (~1300 cm^{-1}) of the I* form significantly upshift relative to the phenolic CH bend (1142 cm^{-1}) and the CO stretch (1240 cm^{-1}) of the A* form. This indicates that the structural change associated with the deprotonation occurs mostly in the phenol moiety of the chromophore. Importantly, a remarkable modulation of the band intensity is observed for the phenolic CH bend of the A* form at ~1142 cm^{-1} at ΔT < 1 ps. At ΔT = 0.1 ps, for instance, the vibrational band exhibits the largest relative intensity that is almost 3 times larger than the adjacent CO stretch mode at 1240 cm^{-1}. In contrast, at 0.2 ps (red spectrum), the intensity of the phenolic CH bend decreases and becomes comparable with the intensity of the adjacent band. Then, the band intensity again increases up to 0.35 ps and decreases at 0.5 ps (red spectrum). Actually, the FT amplitude (Figure 4A, top) shows a large oscillatory modulation with ~104 cm^{-1} frequency (period: 0.32 ps) and ~0.5 ps dephasing time. On the other hand, periodic oscillation of the frequency of the phenolic CH bend (Figure 4B, top) is not very clear with the experimental error of the present measurement, although slight modulation may be recognized. In Figure 4, the FT amplitudes and the frequencies of other vibrations of the A* form are also compared. For the phenolic CO stretch (~1240 cm^{-1}), the amplitude monotonically decreases with ΔT due to the depopulation of the A* form by the ESPT, whereas the amplitudes of exocyclic C═C−C bend

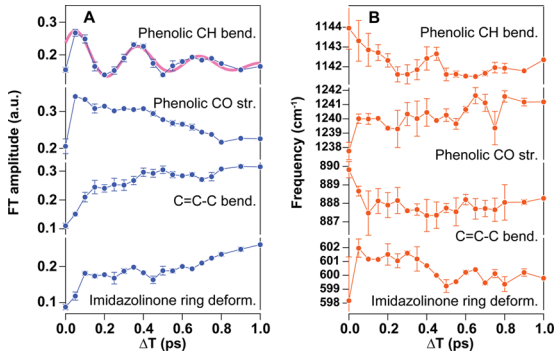

Figure 4. Temporal profiles of the FT amplitudes (A) and the frequencies (B) of the vibrational bands determined by Gaussian fit. The best fit to the oscillating amplitude of the phenolic CH bend is also plotted.

(~888 cm^{-1}) and imidazolinone ring vibrations (~601 cm^{-1}) increase because they overlap with the I*-form vibrations that grow with the ESPT. In the present TR-ISRS data, we consider within the experimental error that none of the frequencies of these modes of the A* form shows oscillation. We observed clear oscillatory modulation only for the one vibration, i.e., phenolic CH bend. The observed modulation frequency coincides with the frequency of the low-frequency band (105 cm^{-1}) found in the pump−probe spectroscopy (Figure 2A). Therefore, the observed amplitude oscillation of the phenolic CH bend clearly indicates the anharmonic vibrational coupling[27,28] between this high-frequency vibration and the low-frequency mode at 105 cm^{-1}, which is coherently excited by the actinic pump. A similar modulation frequency (120 ± 20 cm^{-1}) was reported in the previous FSRS study.[17]

According to our formulation based on the anharmonic coupling (SI), the amplitude modulation arises from the third-order coupling proportional to $x^2Q_{\mathrm{CH\ bend}}$. With this coupling, the shift of the equilibrium structure along the phenolic CH bend coordinate ($Q_{\mathrm{CH\ bend}}$) is induced by excitation of a low-frequency mode (x). In the tightly packed situation around the chromophore in the protein, the vibrational potential of the high-frequency mode would be significantly deformed, inducing the anharmonic terms. It was suggested that the low-frequency motion that changes the distance between the surrounding residues and the phenol moiety of the chromophore anharmonically couples to the high-frequency vibrations of the A* form.[17] The relevant vibration, such as phenolic wag, is a possible assignment for the observed low-frequency mode. This low-frequency mode is the mode that was claimed to mediate the ESPT of GFP.[17]

When the observed low-frequency mode involves the hydrogen-bond change around the phenol moiety of the chromophore, the central question is whether the low-frequency vibration significantly affects the ESPT efficiency as proposed.[17] If this is the case, it is expected that the coherent low-frequency motion induced by photoexcitation modulates the initial ESPT rate and that the early time production of the I* form shows the corresponding low-frequency modulation. In Figure 5, the amplitude of the ~1295 cm^{-1} band of the I* form is plotted in comparison to the low-frequency modulation of the phenolic CH bend of the A* form. While the A* form clearly shows the coherent ~104 cm^{-1} vibrational motion, the growth of the I* form is almost monotonic, although very small modulation might exist (see SI for its Fourier analysis and further discussion). This

DOI: 10.1021/jacs.5b11038
J. Am. Chem. Soc. 2016, 138, 3942−3945

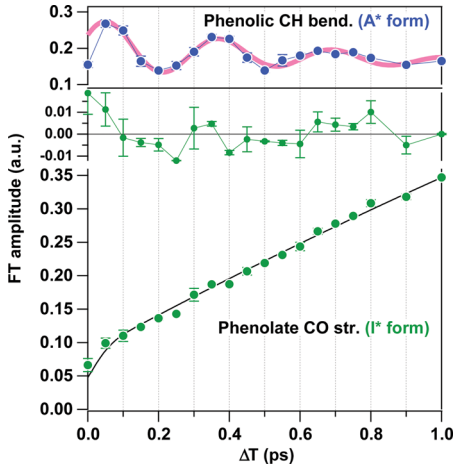

Figure 5. Temporal change in the FT amplitude of phenolate CO stretch of the I*form (lower). The fit with an exponential function (black line) convoluted with the instrumental response of 110 fs and the residual are also plotted. The oscillatory feature of the phenolic CH bend of the A* form (upper) is shown for comparison.

indicates that the ~104 cm^{-1} motion does not have a large effect on the ESPT efficiency in GFP. Therefore, even if the low-frequency coherent motion mediates the ESPT, the contribution is small, and it does not play a predominant role in the ESPT, at least at room temperature.

Upon the deprotonation of the chromophore, the proton travels via water and Ser205 to Glu222 in the ESPT of GFP.[14,15,29] Therefore, the overall reaction coordinate consists of all intermolecular and inter-residue vibrational modes in the hydrogen-bond chain of chromophore-water-Ser205-Glu222. Although some intermolecular modes involving the chromophore are coherently photoexcited, other modes which predominantly involve Ser205 and Glu222 are not, but they are thermally, or incoherently, fluctuating. Given that those thermal motions contribute to the ESPT process, it is unlikely that the initially generated coherence of a specific low-frequency motion largely and directly modulates the efficiency of the I* formation, particularly at room temperature. The monotonic growth of the I* form suggests that the ESPT is not driven solely by one single low-frequency mode of the chromophore but rather involves thermally excited motions, including those of the hydrogen-bond chain, to transfer a proton.

■ ASSOCIATED CONTENT

Supporting Information

The Supporting Information is available free of charge on the ACS Publications website at DOI: 10.1021/jacs.5b11038.

Experimental methods and data (PDF)

■ AUTHOR INFORMATION

Corresponding Author

*tahei@riken.jp

Present Address

[‖]Department of Chemistry and Applied Chemistry, Graduate School of Science and Engineering, Saga University, Saga, 840-8502, Japan

Author Contributions

[⊥]These authors contributed equally.

Notes

The authors declare no competing financial interest.

■ ACKNOWLEDGMENTS

This work was partly supported by KAKENHI, Grant-in-Aid for Scientific Research (A) (no. 25248009) and Grant-in-Aid for Scientific Research on Innovative Areas (no. 25104005), from MEXT/JSPS. We thank Ms. Yumi Sagara at Toho University for the preparation of GFP.

■ REFERENCES

(1) Tsien, R. Y. *Annu. Rev. Biochem.* **1998**, *67*, 509.
(2) Giepmans, B. N. G.; Adams, S. R.; Ellisman, M. H.; Tsien, R. Y. *Science* **2006**, *312*, 217.
(3) Kerppola, T. K. *Chem. Soc. Rev.* **2009**, *38*, 2876.
(4) Day, R. N.; Davidson, M. W. *Chem. Soc. Rev.* **2009**, *38*, 2887.
(5) Craggs, T. D. *Chem. Soc. Rev.* **2009**, *38*, 2865.
(6) van Thor, J. J. *Chem. Soc. Rev.* **2009**, *38*, 2935.
(7) Meech, S. R. *Chem. Soc. Rev.* **2009**, *38*, 2922.
(8) Chattoraj, M.; King, B. A.; Bublitz, G. U.; Boxer, S. G. *Proc. Natl. Acad. Sci. U. S. A.* **1996**, *93*, 8362.
(9) Yang, F.; Moss, L. G.; Phillips, G. N. *Nat. Biotechnol.* **1996**, *14*, 1246.
(10) Ormo, M.; Cubitt, A. B.; Kallio, K.; Gross, L. A.; Tsien, R. Y.; Remington, S. J. *Science* **1996**, *273*, 1392.
(11) Brejc, K.; Sixma, T. K.; Kitts, P. A.; Kain, S. R.; Tsien, R. Y.; Ormo, M.; Remington, S. J. *Proc. Natl. Acad. Sci. U. S. A.* **1997**, *94*, 2306.
(12) Winkler, K.; Lindner, J.; Subramaniam, V.; Jovin, T. M.; Vöhringer, P. *Phys. Chem. Chem. Phys.* **2002**, *4*, 1072.
(13) Kennis, J. T.; Larsen, D. S.; van Stokkum, I. H.; Vengris, M.; van Thor, J. J.; van Grondelle, R. *Proc. Natl. Acad. Sci. U. S. A.* **2004**, *101*, 17988.
(14) van Thor, J. J.; Zanetti, G.; Ronayne, K. L.; Towrie, M. *J. Phys. Chem. B* **2005**, *109*, 16099.
(15) Stoner-Ma, D.; Jaye, A. A.; Matousek, P.; Towrie, M.; Meech, S. R.; Tonge, P. J. *J. Am. Chem. Soc.* **2005**, *127*, 2864.
(16) van Thor, J. J.; Ronayne, K. L.; Towrie, M.; Sage, J. T. *Biophys. J.* **2008**, *95*, 1902.
(17) Fang, C.; Frontiera, R. R.; Tran, R.; Mathies, R. A. *Nature* **2009**, *462*, 200.
(18) Fujiyoshi, S.; Takeuchi, S.; Tahara, T. *J. Phys. Chem. A* **2003**, *107*, 494.
(19) Cerullo, G.; Lueer, L.; Manzoni, C.; De Silvestri, S.; Shoshana, O.; Ruhman, S. *J. Phys. Chem. A* **2003**, *107*, 8339.
(20) Takeuchi, S.; Ruhman, S.; Tsuneda, T.; Chiba, M.; Taketsugu, T.; Tahara, T. *Science* **2008**, *322*, 1073.
(21) Liebel, M.; Kukura, P. *J. Phys. Chem. Lett.* **2013**, *4*, 1358.
(22) Kraack, J. P.; Wand, A.; Buckup, T.; Motzkus, M.; Ruhman, S. *Phys. Chem. Chem. Phys.* **2013**, *15*, 14487.
(23) In the present TR-ISRS data, the high-frequency vibrational modes (> 1400 cm^{-1}) are less pronounced when compared to the reported FSRS spectrum of the A* form.[17] This is attributed to the difference in the resonance condition: The FSRS data were measured with the resonance enhancement through the $S_n \leftarrow S_1$ transition while the TR-ISRS data was obtained under a rigorous resonance condition with the $S_1 \rightarrow S_0$ transition.
(24) Bell, A. F.; He, X.; Wachter, R. M.; Tonge, P. J. *Biochemistry* **2000**, *39*, 4423.
(25) Gnanasekaran, R. *Chem. Phys. Lett.* **2013**, *587*, 61.
(26) Kondo, M.; Heisler, I. A.; Stoner-Ma, D.; Tonge, P. J.; Meech, S. R. *J. Photochem. Photobiol., A* **2012**, *234*, 21.
(27) Hoffman, D. P.; Ellis, S. R.; Mathies, R. A. *J. Phys. Chem. A* **2014**, *118*, 4955.
(28) Valley, D. T.; Hoffman, D. P.; Mathies, R. A. *Phys. Chem. Chem. Phys.* **2015**, *17*, 9231.
(29) Lill, M. A.; Helms, V. *Proc. Natl. Acad. Sci. U. S. A.* **2002**, *99*, 2778.

DOI: 10.1021/jacs.5b11038
J. Am. Chem. Soc. 2016, 138, 3942−3945